**Citation**: G. Indira Devi, D. Madhavi. Detection and classification of diabetic retinopathy through identification of blood vessel thickness using FOFF & ML classifiers. *Journal of Harbin Institute of Technology (New Series)*. DOI: 10.11916/j.issn.1005-9113.2024039.

# Detection and Classification of Diabetic Retinopathy Through Identification of Blood Vessel Thickness Using FOFF& ML Classifiers

*G.Indira Devi*[1*] *and D.Madhavi*[2]

(*1. Electronics and Communication Engineering, Anil Neerukonda Institstute of Technology and Science, Visakhapatnam 531162, Andhra Pradesh, India;*
*2. Department of Electrical, Electronics and Communications Engineering, GITAM University, Visakhapatnam 530045, Andhra Pradesh, India*)

**Abstract**: Diabetes is a significant issue in the medical field. The detection and identification of the human eye diseases caused by excessive blood sugar levels in diabetes mellitus are important. The main objective of this study is to propose a viable solution for diagnosis using fundus images. This study presents a stage by stage implementation methodology. The original fundus image is first preprocessed, then the blood vessels are segmented, and finally the features are extracted and classified. This work uses an effective way to introduce a meta-heuristic algorithm. Blood Vessel Segmentation (BVS) is vital in DR(Diabetic Retinopathy) detection; hence, this research proposes a Firefly-Optimized Frangi based Filter (FOFF). Categorizing the disease is the last procedure. The classifier K-Nearest Neighbour (KNN) has an accuracy of 91.62%, while the SVM does well with an accuracy score of 95.54%.

**Keywords**: diabetic retinopathy; firefly algorithm; optimized Frangi filter; KNN; SVM
**CLC number**: TP391.4, R774.1 **Document code**: A **Article ID**: 1005-9113(2024)00-0000-13

## 0 Introduction

Segmentation of blood vessels on retinal imaging can help ophthalmologists diagnose a wide range of eye disorders. To fully analyze the principal blood vessels and their sub branches thorough blood vessel segmentation is required[1]. Presently, clinicians manually classify blood vessels from their prior experiences, but it is inaccurate and prone to bias the treatment[2]. The retinal blood vessels segmentation through automation process is consequently critical[3]. Gaussian filter approach was used by Chaudhuri et al.[4] initially to segment blood vessels. Li et al.[5] proposed an approach that combined a threshold and a matching filter with multiscale for segmentation purpose. Kaur et al.[6] developed a technique for segmentation using a Gray-level Co-occurrence Matrix (GCM) and a Gabor filter. Tian et al.[7] employed the multiscale 2D Gabor wavelet to assess blood vessels. An extended matcher was proposed by Singh[8]. Cruz-Aceves et al.[9] used segregated blood vessels and a Gabor Filter (GF) with multi-scale and a multi-objective optimization-based thresholding technique.

The blood vessels profile and structure were improved by using the GF and function with Gaussian distribution derivatives suggested in Ref. [10]. The segmentation of retinal vessels requires improvement, Singh et al.[11] suggested a technique with matched filtering based on the Gumbel probability distribution function. This approach can preserve the initial vessel structures, but every pixel must be analyzed, the computing effort and the time for segmentation are greatly increased. Frangi et al.[12] employed Hessian matrix to extract the different directions of images. Using the features of LoG and matched filter, Kumar et al.[13] identified retinal images blood vessels while discarding inaccurate classification of non-vessel structure pixels. Fathi et al.[14] developed segmentation with multiscale for vascular structure using the wavelet transform's continuity function.

Received 2024-04-19.
* Corresponding author: G. Indira. Devi, Ph.D Scholar. Email: gedela.indira@ gmail.com.

Zhao et al.[15] proposed a regional growth based algorithm. Rezaee et al.[16] proposed a technique for segmenting retinal vessels which used skeletonization, adaptive filtering and fuzzy entropy. A method for improving fine blood vessels through vascular space and axial ratio was published in Ref. [17]. Zhao et al.[18] used vessel tracking technologies to identify unique local features. However, due to branching, they are not able to get tracking continuously, resulting in inappropriate segmentation. Rodriguez et al.[19] described a method for identifying optic discs using wavelet transforms and mathematical morphology.

Based on the blood vessel features, retinal images were distinguished using the recommended method. Using morphology and topology operations, Rodriguez et al.[20] extracted the vascular tree's pixels and found topological vessel properties and linkages. Câmara Neto et al.[21] published a vascular identification method for retinal images. Initially, generic vascular segmentation was used in this technique. Second, morphological reconstruction and curvature analysis were used to segment the vessels with greater accuracy. Morphology-based operations remove noise quickly, very well, and efficiently. They do, however, significantly depend on the selection of structural elements. Despite significant advancements, blood vessel segmentation is still a challenging problem because of various limitations related to image quality, variability in vessel appearance, dataset constraints, algorithmic complexity, computational demands, and clinical integration.

This work proposes a technique for blood vessels segmentation of fundus photographs found on the Frangi filter with firefly optimization technique. The green channel of the original RGB fundus image was separated by initial processing. Next, blood vessel health was improved by CLAHE (Contrast Limited Adaptive Histogram Equalization). Third, blood vessels segmentation is carried out. Lastly, KNN and SVM classifiers are used to perform classification.

## 1 Related Work

Diabetic Retinopathy (DR) has four main primary treatments for blindness around the globe. Research indicates that severe retinopathy causes blindness in as many as 37.4% of the population in China and India[22]. The vessel structure of the eye is extensively disseminated. Thus, in the majority of diabetics, abnormalities of the eyes are connected with blood vessels. Liu et al.[23] used a driving dataset and suggested a heterogeneous neural network that combined the benefits of semantic information extraction from a Convolutional Neural Network (CNN) and long-range spatial feature minimizing of transformer network architectures. The obtained accuracy is 93.8%, sensitivity is 61% and F1 score is 81.6%. There is a need in improving all the parameters to improve the diagnosis.

Zhu et al.[24] proposed a Laplacian pyramid model for image enhancement and improved matching filter algorithm for image segmentation. For this purpose, DRIVE dataset is utilized and achieved results with 74.6 % sensitivity, 97.3% specificity and an F1 score of 84.5%. There is a need to proceed with deep learning algorithms in order to get the improved detection accuracy using the retinal image database.

Singh et al.[25] proposed five deep learning-based networks for segmentation of the retinal blood vessel structure, an enhanced customized R2-ATT U-Net deep learning network. The result shows an accuracy of 97.1%. Khanna et al.[26] proposed a CNN-LTSM model for prediction of diabetic retinopathy. The results obtained using the model showed an accuracy of 95.4%, F1 score is 96.8% and sensitivity is 95.6%. Khanna et al.[27] designed a new model, i.e. PlaNet for detection of plant leaf disease. This model can be studied and implemented for retinal images. The results obtained in detection of lead disease with an accuracy of 97.9%. The deep CNN architectures are utilized in various detection process. Khanna et al.[28] utilized CNN-LTSM model detection of Covid-19 and achieved an accuracy of 99.7%.

Advancements in image processing technology have increased with the rise of artificial intelligence and meta-heuristic algorithms. The author introduced the assessment method of Fundus Camera Images (FCI), based on the SMOA (Spider Monkey Optimization Algorithm) in Ref.[29]. Traditional threshold segmentation approaches primarily rely on the OTSU (an automatic image thresholding algorithm) and an unsupervised learning technique that uses the highest variance across classes to separate images. The OTSU approach for segmenting DR vascular pictures using a variety of criteria is computationally demanding and difficult to apply in practice. Most of the scholars have proposed population optimization procedures to handle multi-threshold difficulties as a solution to this

problem. This study examines the Rim-One FCI dataset using the OD(Optic Disc) and stereo picture. Then the SMOA's efficiency is compared to various heuristic algorithms. SMOA provides an accuracy of 94.2%.

The optimization algorithms are combined to improve the detection accuracy. Deng et al.[30] proposed particle swarm optimization algorithm and salp swarm algorithm for segmentation of diabetic retinal images. The metrics, such as SSIM, FSIM, sensitivity, specificity, and accuracy, are identified. The accuracy obtained is 94.7%, specificity is 98.5% and sensitivity is 74.4%. The author compared the PMSSA model with other optimization techniques, such as Salp Swarm Algorithm (SSA), Whale Optimization Algorithm (WOA), Social Spider Optimization (SSO), Particle Swarm Optimization (PSO).

Ant Colony Optimization (ACO) was used to segment the fundus pictures with numerous thresholds and ACO's specific pheromone updating technique improves segmentation accuracy[31]. This method was tested with the Rim-One dataset, resulting in 24.3% of an average overlapping error of the cup segmentation and an Area Under the Curve (AUC) of 0.7957 when employing the cup-to-disc ratio for glaucoma evaluation. Al-Rawi et al.[32] segmented the fundus picture of the DR using a Genetic Process (GA). DRIVE dataset is utilized for the designed model. The Receiver-Operating characteristic Curve (ROC), the receiver operating curve serves as a fitness function for the genetic algorithm. To assess the performance of improved matched filter, the maximum average accuracy is found to be 94.22%, while the average area under the ROC is 95.82%. From the above findings, the segmentation accuracy need to be further improved by proposing good model for blood vessel segmentation. By combining optimization with machine learning, provide good result can be achieved, which is considered in the paper.

## 2 Materials and Method

To evaluate the vessel detection techniques, pictures are extracted from the publicly available DRIVE database[33]. The DRIVE dataset is often used to assess the proposed methodology for vascular segmentation because it allows for human segmentation. 10 retinal fundus images are taken from the DRIVE, and for each image, industry benchmarks are compared with criteria, such as sensitivity and specificity findings. In Fig. 1, the suggested framework is displayed. In Fig. 2, the DRIVE dataset example is displayed.

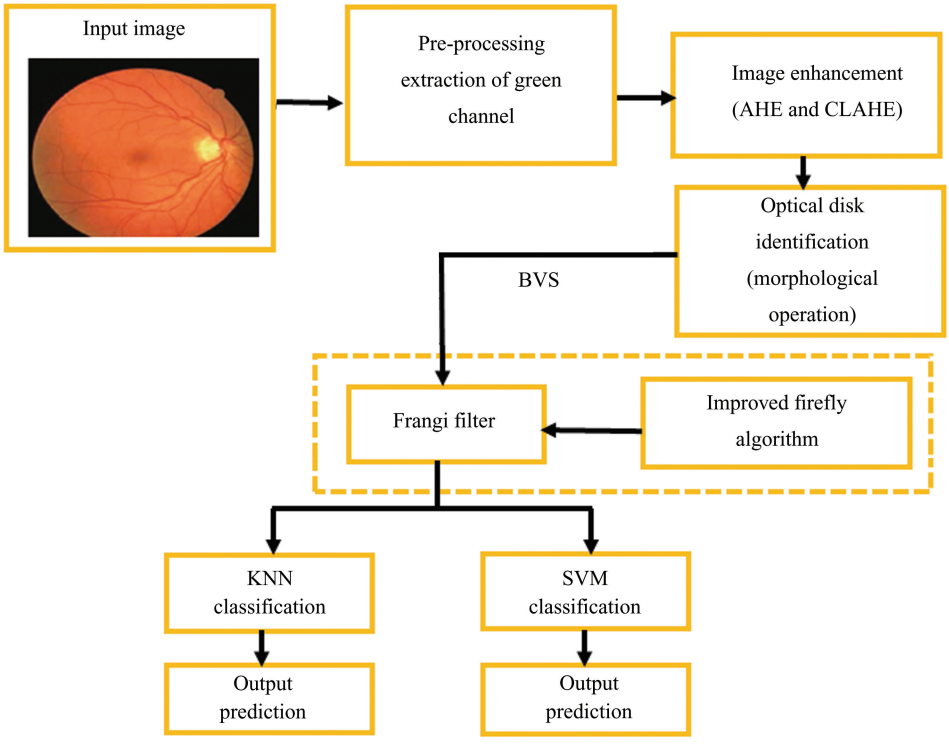


**Fig.1 Proposed model**

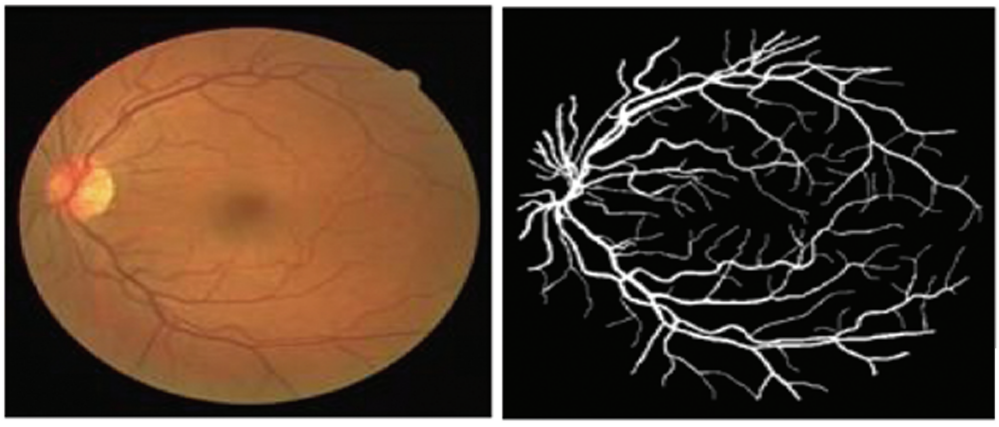

(a) A ground truth image (b) A source image

**Fig.2 Drive dataset containing ground truth and source images**

## 2.1 Pre-Processing

Fundus retinal images are usually in RGB format, which needs to be converted. This simplifies data processing for diagnosis of lesions, for which single-channel images are created. The Red (R), Green(G), and Blue (B) channels are extracted and the images of them are as shown in Fig. 3. The G-channel image's background and blood vessels contrast dramatically. Pre-processing was therefore applied to the G-channel image.

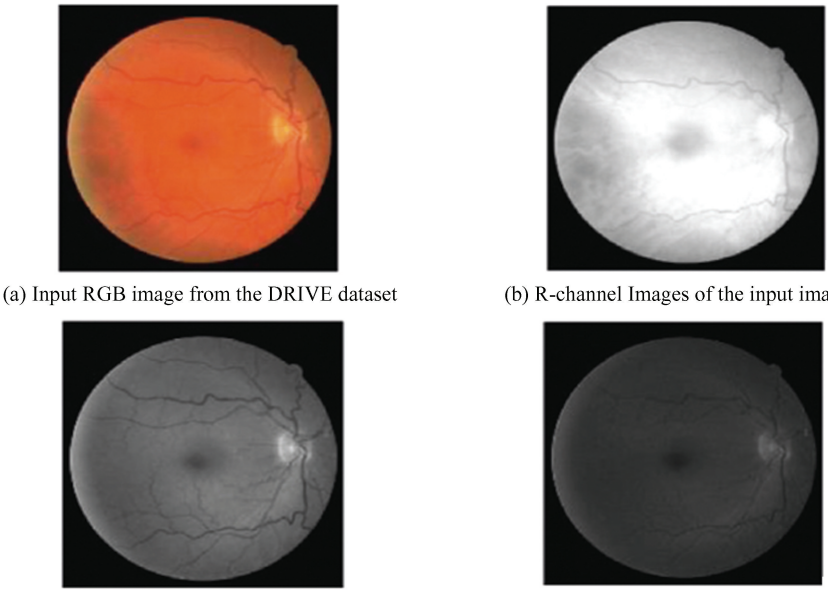

(a) Input RGB image from the DRIVE dataset (b) R-channel Images of the input image

(c) G-channel Images of the input image (d) B-channel Images of the input image

**Fig. 3 RGB conversion of a color picture**

## 2.2 Image Enhancement

The augmentation of a retinal image can assist in differentiating blood vessels from surroundings. The histogram equalization technique applied to a particular image can enhance the brightness of each individual element, expanding the intensity range of the retinal image. The fundus retinal images do not show the required augmentation of blood vessels due to the black and low brightness of the vascular region. This makes the global histogram equalization approach inadequate.

Adaptive Histogram Equalization (AHE) enhances the histogram of every pixel in an image by finding the transformation function of each neighboring pixel's domain. To get additional information, AHE is more suited for enhancing local contrast and picture edges. In retinal vascular imaging, AHE may improve the noise surrounding tiny blood vessels while increasing contrast[34]. It is imperative to have the CLAHE technique in conjunction with retinal vascular enhancement, since it has the ability to inhibit noise amplification[35].

Furthermore, the CLAHE method uses a simple algorithm to discover only one amplitude limit parameter. Fig. 4(a) illustrates how the CLAHE algorithm is processed. The outcomes of the enhancement in Fig. 4 were compared. The AHE algorithm enhanced the small blood vessels and enhanced the background noise in the image. This feature led to the unequal brightness distribution in the photograph. On the other hand, the CLAHE algorithm significantly decreased noise interference and enhanced the contrast between the background and the foreground blood vessels.

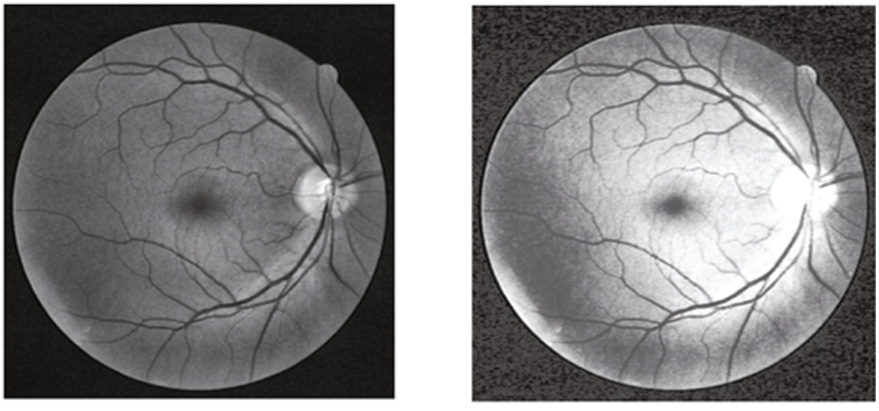

(a) Image using CLAHE (b) Image using histogram equalization

**Fig.4 Image enhancement**

### 2.3 Optic Disk Identification and Extraction from Retina

The benefits of using an automated system which recognize the early warning signs of this disease automatically have been well-examined and shown to be favorable. Consequently, the OD segmentation plays a critical role in most of the algorithms used to extract fundus features, making the Optic Disc(OD) essential in the construction of DR diagnosis automated expert systems. Morphological operations are employed to determine the OD. Once the OD has been detected, the noise interference in the backdrop of the image is eliminated.

During dilatation, the elements of the eye are used to every binary visual pixel. Each time the origin of a structural element is joined with binary pixels, the corresponding binary image pixels are altered, and the structural element as a whole is completed. The output, which had a zero initialization, is a binary image that contains the logical addition results. When using structural erosion, the element also moves across every pixel in the image.

The morphological operations are represented mathematically as Eqs.(1) and (2).

$$D_{\mathrm{I}} = I \circ \otimes E_{\mathrm{s}} \quad (1)$$

$$E_{\mathrm{I}} = I_{\mathrm{o}} \ominus E_{\mathrm{s}} \quad (2)$$

where $I_{\mathrm{o}}$ is original input image , $E_{\mathrm{s}}$ is a structuring element, $D_{\mathrm{I}}$ is the dilated image, and eroded image is given as $E_{\mathrm{I}}$ .

An open technique can be used to remove bright areas of the image that are smaller than structural parts.

$$O_I = I_o \circ E_s \quad (3)$$

In Eq. (3) 'o' represents the morphological opening operation. Eq. (3) is shorthand notation for applying the morphological opening operation on image $I_o$ with structuring element $E_s$.

Blood vessels with an optic disk border are identified and separated from the G-channel because the G-channel is suited for vessel recognition in the retinal fundus image. Fig. 5 represents the OD region identification and extraction.

### 2.4 Blood Vessel Segmentation

Blood Vascular Segmentation (BVS) is carried out following the identification of the optical disk. BVS suggested an improved Frangi filter in response to this. The enhanced firefly algorithm is used to optimize the filter. The achievement of improving filters may have a substantial influence on how well vessels are segmented. The most popular techniques for improving vessels rely on the image's differential information and second-order derivative. Since the vessels come in a range of sizes, the research is frequently conducted on a number of scales.

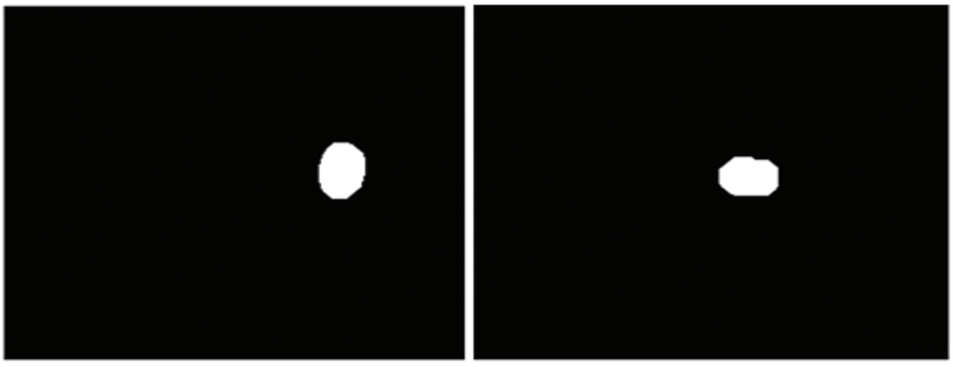

(a) (b)

**Fig. 5 (a) & (b) OD region identification and extraction from two input images**

If $I_o(x,y)$ is the original image, then the Hessian (scaled-down) of $I_o(x,y)$ is represented by Ref.[36].

$$H_e(x,y,s) = s^2 I_o(x,y) \cdot \frac{\partial^2}{\partial x \partial y} Gf(x,y,s) \quad (4)$$

$$Gf(x,y,s) = (2\pi s^2)^{-1/2} \exp\left(-\frac{x^2+y^2}{2s^2}\right) \quad (5)$$

Here $Gf(x,y,s)$ is the Gaussian distribution function which has $k$ kernel size. Changes to the kernel size can account for different picture spacing for different sizes. Examining the Hessian Eigen Values (HEV) sizes and signs within the context of vessel detection makes intuitive sense. By analyzing the magnitudes and indications of the HEV, the local structure of the image can be improved. The Eigen Value decomposition technique is used to derive the Hessian matrix Eigen Values by ,i.e., $eig\, H_e(x,y,s) \rightarrow \lambda_i, i = 1,2$.The Eigen values obtained i.e., $|\lambda_1| \leqslant |\lambda_2|$.

Furthermore, when the vessels are luminous tubular shapes in three dimensions, negative values are observed. By employing this sign data as a reliability analysis, the possibility of additional components in the image is excluded. Several vesselness functions are obtained based on the Eigen Values of the Hessian Matrix (HM). Frangi et al.[12] defined the vesselness function $V_{\text{frangi}}$ by utilizing the ratio of Eigen Values.

$$V_{\text{Frangi}} = \begin{cases} 0, \text{if } \lambda_2 > 0, \\ \exp\left(-\dfrac{\left(\dfrac{\lambda_1}{\lambda_2}\right)^2}{2\delta^2}\right)\left(1-\exp\left(-\dfrac{\lambda_1^2+\lambda_2^2}{2\omega^2}\right)\right), \text{otherwise} \end{cases} \quad (6)$$

The distinct focus of the functions on $\lambda_1$ and $\lambda_2$ diminishes response consistency and heightens their sensitivity to contrast in images. Furthermore, with lower values of $\lambda_2$, the function's response is not up to par. As such, it is quite vulnerable to picture noise. To overcome this, Deng et al.[30] suggested an improved vesselness function $V$ as in Eq. (7), in which $\lambda_p$ is defined as below.

$$V = \begin{cases} 0, \text{if } \lambda_2 > 0 \\ \lambda_2^2(\lambda_\rho - \lambda_2)\left(\dfrac{3}{\lambda_2+\lambda_\rho}\right)^3, \text{if } \lambda_2 \leqslant \dfrac{\lambda_\rho}{2}, \\ 1, \text{otherwise} \end{cases} \quad (7)$$

$$\lambda_\rho = \begin{cases} \lambda_2 if\, \lambda_2 < \tau \min_{x,y} \lambda_2(x,y,s) \\ \tau \min_{x,y} \lambda_2(x,y,s), \text{otherwise} \end{cases} \quad (8)$$

To ensure the vesselness function robustness over l $\tau$ ower-level magnitudes of $\lambda_2$, the value of $\lambda_2$ is regularized at every level $s$ in this instance. Between [0, 1], which is a cut-off threshold, lies $\tau$. In order to achieve negative eigenvalues, the bright structures against the dark background must be emphasized. Hence, $\lambda_2$ of greater size can be found as $\min_{x,y} \lambda_2(x, y, s)$ .The vesselness function in Eq. (8) is studied at multiple scales. The performance of the filter peak at a scale that almost same as the dimensions of the intended vessel. We integrate the measure of vesselness provided by the filter response at different scales to produce enhanced picture estimation at various scales $I_{\text{enhanced}}(x,y)$ as in Eq.(9).

$$I_{\text{enhanced}}(x,y) = \max_{s_{\min} \leqslant s \leqslant s_{\max}} (V) \quad (9)$$

where the $S_{\min}$ and $S_{\max}$ are the expected sizes of the vessels of interest which define the scale range.

*2.4.1 Improved firefly optimized algorithm*

The attraction between fireflies is irrespective of their sexes, because of their unisex nature. Firefly attraction decreases with increasing distance and is negatively associated with light intensity. The less brilliant firefly will move toward the more brilliant one in any pair that is flashing. If there is not another firefly that is brighter than the one in question, it will

travel at random.

The suggested Firefly Algorithm's (FA) implementation process is as follows.

$S_1$: Create the population of fireflies, $\{x_1, x_2, \cdots, x_n\}$

$S_2$: Determine the brightness of each firefly.

$S_3$: Updates for every firefly.

$S_4$: The intensity of fireflies is represented as $\{I_1, I_2, \cdots, I_n\}$

$S_5$: Selecting the best one at the moment.

$S_6$: Shifting each firefly $I_i (i = 1, 2, \cdots, n)$ toward other brighter fireflies.

$S_7$: Proceed to $S_2$ if the criterion is not met, stop when it is.

*2.4.2 Firefly algorithm parameters*

A distance known as the Cartesian or Euclidean distance is measured between two fireflies $(i, j)$ and their positions $(x_i, x_j)$. $r_{ij}$ is given as follows:

$$(r)_{ij}) = \|x_i - x_j\| = \sqrt{\sum_{k=1}^{d} (x_{i,k} - x_{j,k})^2} \quad (10)$$

where $x_{i,k}$ is the brightness of a firefly, and $k$ is the $k^{\text{th}}$ component of the coordinate $x_i$ of the $i^{\text{th}}$ firefly.

The attractiveness $\beta$ varies with the distance $r$, and

$$\beta = \beta_o \quad (11)$$

where $\beta_o$ is the attractiveness at distance $r = 0$.

A firefly $i$ moves as a result of and is provided by another firefly j that is more enticing (brighter) is given by Eq. (12).

$$X_i^{t+1} = x_i^t + \beta_o e^{-\gamma r_{ij}^2}(x_j^t - x_i^t) + \alpha_t \varepsilon_i^t \quad (12)$$

where $X_i^{t+1}$: The position of ith firefly when time is $t + 1$; $x_i^t$: The position of ith firefly when time is $t$; $\beta_0$: Maximum attractiveness (when distance is zero); $x_j^t - x_i^t$: Vector difference between the positions of firefly $j$ and firefly $i$; $\gamma$: Light absorption coefficient, which controls the decay of attractiveness over distance; $r$: Distance between two fireflies.

The attraction parameter is the basis of the second term in Eq. (12). The third term is referred to as the random term, where $\alpha$ is the randomization parameter and $\varepsilon_i^t$ is a vector of random values.

The vesselness function cannot be calculated without the knowledge of the eigenvalues of the Hessian matrix, $\lambda_2$ and $\lambda\rho$. To enhance the Frangi Filter's performance, these Eigen values are adjusted by the use of firefly optimization.

$$\varphi_{\text{opt}} = \frac{\text{argmax}}{s_{\min}, s_{\max}, k, \tau} \{EV(I_{\text{enhance}}(x, y))\} \quad (13)$$

This optimization is to find the optimal parameters of $\varphi_{\text{opt}}$, such as $s_{\min}$, $s_{\max}$, $k$, $\tau$, to maximize the Eigen values for the enhanced image. The optimal set of parameters produces the best-enhanced version of the image.

The parameters of the Frangi filter will be improved by the proposed firefly optimization. These parameters are continuously adjusted to maximize the objective function. The optimized parameters lead to improvement of the segmentation process. The vesselness function of the filter is tuned so that the segmentation of blood vessels will have good quality of visibility. The Eigen values and the Hessian matrix of the image are optimized and analysed for the blood vessels present in the retinal image. Fig. 6 shows the segmented blood vessels.

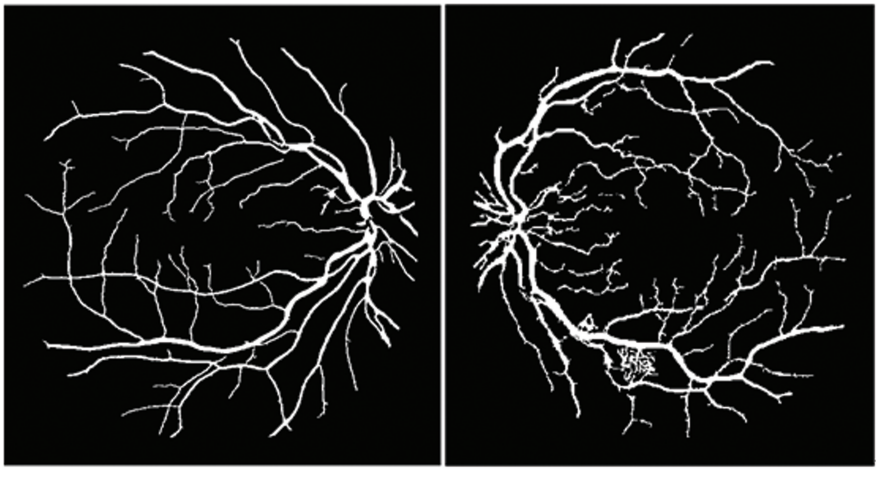

(a) (b)

**Fig. 6 (a)&(b) Segmented blood vessels of two input images**

## 2.5 Feature Extraction

The Gray-Level Co-occurrence Matrix (GLCM) is used for feature extraction of a greyscale image. The GLCM methods determine the frequency of pixel pairings in an image that appear in a given amount and spatial arrangement. This produces a GLCM, from which statistical features describing the texturing of an image are extracted.

One popular texture-based feature extraction technique is GLCM. In order to determine the texture of the pixel-to-pixel connection, this technique applies an operation to the retinal images based on second order statistics. For this process, two pixels are often employed. The GLCM algorithm determines the frequency of intensity combinations of these pixels. Otherwise, this approach shows how frequently pixels couple together. An image's GLCM features are represented as a matrix with $i$-rows and $j$-columns representing the image's gray values.

The elements of the matrix make use of the frequency of the two pixels. The two pixel pairings may be affected differently by the neighbourhood. These matrix members include the second-order statistical probability values. This transient matrix greatly expands at wide intensity levels. This results in a process load which take ages.

Contrast: This statistic uses the contrast between a pixel and its neighbouring pixels to determine how intense an image is overall. When the image is constant, the contrast value is 0.

$$\text{Contrast} = \sum_{i,j} |i-j|^2 p(i,j) \tag{14}$$

Correlation: The correlation value ranges from −1 to 1. The correlation is not taken into account for the constant image. If the value is 1, a picture is positively correlated, and if the value is −1, it is negatively correlated.

$$\text{Correlation} = \sum_{i,j} \frac{(i-\mu i)(j-\mu j)p(i,j)}{\sigma_i \sigma_j} \tag{15}$$

Energy: The energy feature of GLCM is the sum of squared values of the pixels in a picture with $i$-rows and $j$-columns. Energy has a value of 1 for a constant image.

$$\text{Energy} = \sum_{i,j} p(i,j)^2 \tag{16}$$

Homogeneity: The image's diagonal measure of the GLCM elements and the distribution elements' closest pixel values. In the case of the GLCM diagonal element, homogeneity has a value of 1.

$$\text{Homogeneity} = \sum_{i,j} \frac{p(i,j)}{1+|i-j|} \tag{17}$$

## 2.6 Classification

In order to ascertain the stage of Diabetic Retinopathy (DR), vascular properties were obtained. Here, we found the pixel density of the retinal vessels. These features are fed into the KNN and SVM classifiers. The class generated by the KNN and SVM classifiers is used to determine if DR is present.

### *2.6.1 KNN*

One well-known and often-used Machine Learning (ML) technique is KNN (K-Nearest Neighbours). Classification is successfully completed by this method. This method of machine learning is called unsupervised machine learning. The K-NN method is non-parametric for both regression and classification. This method's fundamental idea is to identify data by figuring out which $k$ data points are closest to it. Stated differently, identify the discrepancies between the feedback and the test outcomes, and then adjust the forecast accordingly. The majority of K-NN classifiers use basic Euclidean metrics to determine the separation between samples provided as vector inputs. Fig. 7 represents KNN classification process.

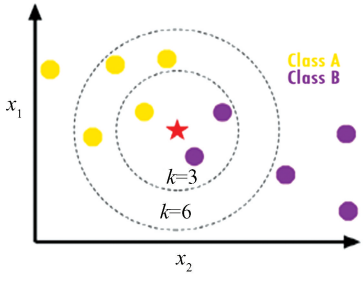


**Fig. 7 KNN classification procedure**

### *2.6.2 SVM*

Originally developed for pattern classification, this technique has recently been extended to other uses, such as regression analysis and distribution estimation. Finding a hyperplane that divides the data points with the least amount of space is the difficult part. The data points are given either positive or negative. SVM generates a hyperplane, or collection of hyper planes, in a high- or infinite-dimensional domain that can be utilized for classification. The process of hyperplane division is shown in Fig.8.

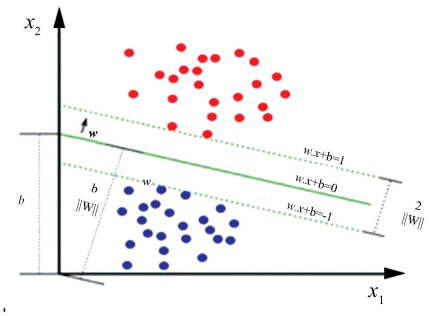


**Fig. 8 SVM classification process**

Considering a set, i.e., $\{(a_1,b_1),(a_2,b_2),\cdots,(a_r,b_r)\}$, is an vector input in $\boldsymbol{A} \subseteq R^n$ and the value of output is $b_i$ , $b_i \in \{1,0\}$ . The class with positive values is termed as '1' and the class with negative value is termed as '0'. The linear function of SVM from the above is Eq. (18).

$$f(a) = (w.a) + k \tag{18}$$

Here $w$ is the normal direction of hyperplane, $b$ is a form of threshold and $k$ is the kernal function. The output based on the threshold is shown in Eq.(19).

$$b_i = \begin{cases} 1, \text{if } (w.a_i) + k \geqslant 0 \\ 0, \text{if } (w.a_i) + k < 0 \end{cases} \tag{19}$$

## 3 Experimental Evaluations

This process of research offers a new approach for the identification of diabetic retinopathy. In this work, the assumption made is that blood vessels have a tubular structure and also form a network branching pattern. The blood vessels assumed to be darker when compared with its surrounding retinal tissues. The purpose of the Frangi filter is to improve tubular structures, such as blood arteries. It makes blood vessels more visible against the backdrop by highlighting portions of the picture that resemble tubes using the Eigen values of the Hessian matrix. The Frangi filter ensures that both big and tiny vessels are increased by detecting vessels of different widths by applying the filter at several scales. The firefly method can efficiently strike a compromise between several goals, such improving vessel structures while reducing artefacts and noise. The results in a vascular segmentation are more accurate. The firefly algorithm is less prone to become stuck in local minima than gradient-based techniques. In order to find the optimal parameter set, it conducts a more comprehensive exploration of the parameter space. By utilising the advantages of both methods, the Frangi filter and the firefly optimisation model improve blood vessel segmentation accuracy. The firefly algorithm's strong parameter optimisation combines with the Frangi filter's capacity to improve tubular structures to produce better segmentation results. More precise and dependable vessel recognition is the outcome of this synergy, which is essential for diagnostic and medical image analysis applications.

This new approach is compared with the traditional algorithms in terms of performance metrics, such as accuracy, precision, and sensitivity. The DRIVE retinal imaging dataset is used to examine the proposed study. DRIVE dataset is one of the most used for performing retinal image segmentation. The images in the dataset are of JPEG format for processing. The resolution of the images is 565×584 mm with RGB colour space. Each image in the dataset is accompanied by a binary mask indicating the vessel locations, created by human experts. This dataset is user friendly and all the new algorithms are tested for improving the analysis of retinal images. The DRIVE dataset has 40 color retinal images divided into training and testing datasets. The testing set includes twenty pictures, mask images and manually detected vessel structures, often known as ground truth images. Fig. 9 shows the results obtained for input image used in Fig.1.

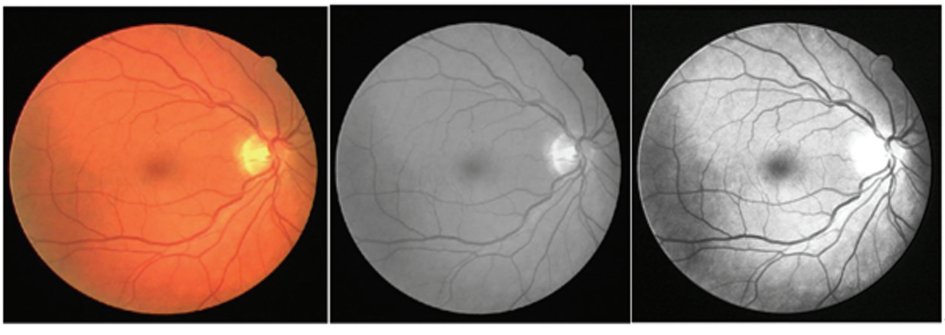

(a) Input RGB image (b) G channel extracted image (c) Enhanced CLAHE image

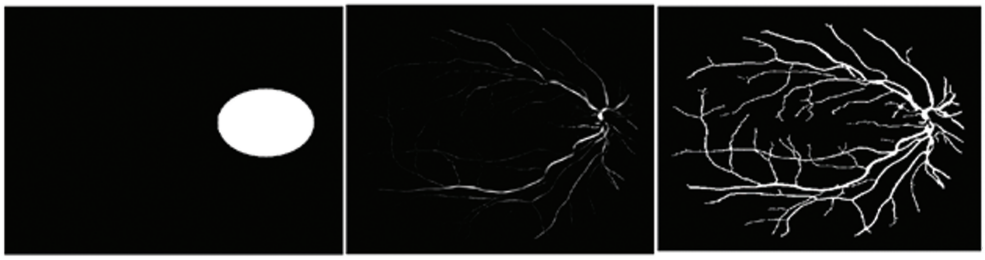

(d) Image of optical disk extraction (e) Output of BVS using Frangi filter (f) Output after applying FOFF for BVS

**Fig. 9 Results of retinal blood vessel segmentation for input image**

The evaluated parameters are sensitivity, accuracy, and precision. All of these obtained by the True Positive (TP), True Negative (TN), False Positive (FP), and False Negative (FN). Accuracy is one of the common measures used to assess the effectiveness of the output. It shows how well the machine recognizes the pixels background and the vessel structure. Mathematically, they are written as follows.

$$\text{Accuracy} = \frac{TP + TN}{TP + TN + FP + FN} \tag{20}$$

$$\text{Sensitivity} = \frac{TP}{TP + FN} \tag{21}$$

$$\text{Precision} = \frac{TN}{FP + TN} \tag{22}$$

Table 1 shows the parameters values obtained using FOFF and KNN classifier for various input images. The proposed method is tested by providing 5 different input images and results are evaluated. The results evaluated using FOFF and SVM classification model is shown in Table 2.

**Table 1 Evaluated parameters for 5 images using FOFF-KNN**

| Images | Accuracy(%) | Sensitivity(%) | Precision(%) |
|---|---|---|---|
| Image 1 | 90.62 | 95.83 | 93.19 |
| Image 2 | 91.84 | 96.25 | 93.23 |
| Image 3 | 92.22 | 94.91 | 91.32 |
| Image 4 | 92.43 | 95.93 | 92.92 |
| Image 5 | 93.92 | 95.94 | 93.13 |
| Average | 91.20 | 95.77 | 92.76 |

**Table 2 Evaluated parameters for 5 images using FOFF-SVM**

| Images | Accuracy(%) | Sensitivity(%) | Precision(%) |
|---|---|---|---|
| IImage 1 | 96.0 | 99.81 | 94.73 |
| IImage 2 | 95.0 | 99.12 | 94.03 |
| Image 3 | 96.0 | 98.95 | 93.92 |
| Image 4 | 95.0 | 99.74 | 94.03 |
| Image 5 | 96.0 | 99.63 | 94.54 |
| Average | 95.6 | 99.42 | 94.37 |

From Table 1 and Table 2, the results show that the performance of SVM classifier is better when compared to KNN classifier. The difference in accuracy rate is around 4%. The parameters, such as sensitivity and precision, also improved by using the SVM classifier. When compared to existing methodologies, the proposed methodology in this research yields encouraging results, which are presented in Table 3.

Segmenting retinal blood vessels is primarily concerned with distinguishing each pixel as a vascular pixel. The segmented image output obtained using the proposed method is compared to the original ground truth image. To see the effectiveness of the model, confusion matrix is used. Figs.10 and 11 illustrate the confusion matrix.

**Table 3 Parameters comparison of different techniques proposed by different authors**

| Author& Year | | Dataset | Accuracy(%) | Sensitivity(%) | Precision(%) |
|---|---|---|---|---|---|
| Panda et al.[37] | | DRIVE | 95.03 | 99.21 | 68.24 |
| Zhang et al.[38] | | DRIVE | 95.12 | 97.1 | 79.73 |
| Pandey et al.[39] | | DRIVE | 95.53 | 96.2 | 80.31 |
| Aguirre-Ramos et al.[40] | | DRIVE | 92.64 | 96.05 | 72.25 |
| Rocha et al.[41] | | DRIVE | 94.83 | 95.72 | 83.32 |
| Proposed Method | KNN(FOFF) | DRIVE | 91.67 | 96.85 | 92.93 |
| | SVM(FOFF) | DRIVE | 95.52 | 99.72 | 94.74 |

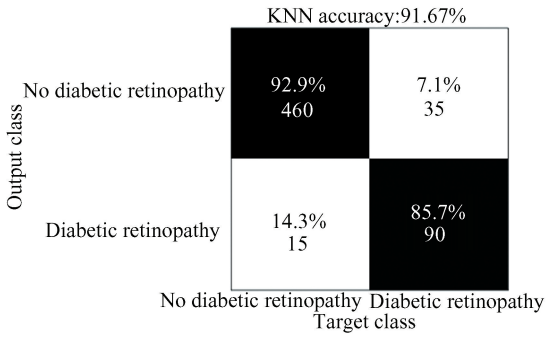


**Fig.10 KNN classifier confusion matrix**

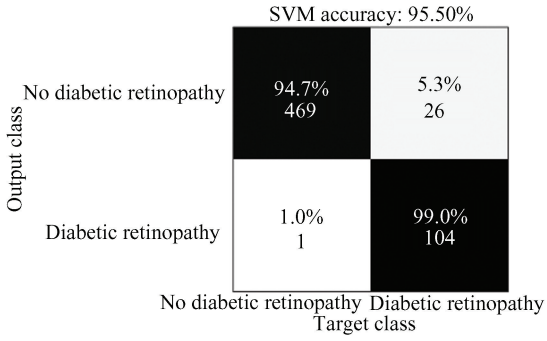


**Fig. 11 SVM classifier confusion matrix**

The proposed model is only implemented on one type of dataset. The model need to be further implemented on various retinal image dataset to prove the validity of results. If the model shows good results on different datasets, it can be used in real time medical fields.

## 4 Conclusions

An ophthalmologist detects diabetic retinopathy using automated procedures for the evaluation of the DR based on computerized blood vessel segmentation of retinal pictures. For this work, the blood vessels of the retina were extracted using pictures obtained from the DRIVE database. Deep research on diabetic retinopathy requires the extraction of vascular structure features. Furthermore, the formation of vessels aids in the determination of the severity and stage of diabetic retinopathy. A unique classification approach for retinal blood vessels is developed using FOFF-KNN and FOFF-SVM. On the truly effected images, the model is tested to demonstrate its efficiency over the models in use. When the proposed model is tested in DRIVE dataset, the results are evaluated with an accuracy of 95.52%, sensitivity of 99.72% and precision of 94.74%. The optic disk interference cause disturbance in vessel segmentation, and the level of blood vessel visibility becomes low for detecting the small set of vessels. Further to improve the accuracy of segmentation, the optic disk removal techniques need to be improved. The vessels which are interlinked and connected to main vessel need to be investigated.

## References

[1] Niemeijer M, Staal J, Van Ginneken B, et al. Comparative study of retinal vessel segmentation methods on a new publicly available database. Proceedings of Medical Imaging 2004: Image Processing. Bellingham: Spie Digital Library, 2004: 5370. DOI:10.1117/12.535349.

[2] Khanduzi R, Sangaiah A K. A fast genetic algorithm fora critical protection problem in biomedical supply chain networks. Applied Soft Computing, 2019, 75: 162 - 179. DOI: 10.1016/j.asoc.2018.11.010.

[3] Al-Turjman F, Nawaz M H, Ulusar U D. Intelligence in the Internet of medical things era: A systematic review of current and future trends. Computer Communications, 2019, 150:644-660. DOI:10.1016/j.comcom.2019.12.030.

[4] Chaudhuri S, Chatterjee S, Katz N, et al. Detection of blood vessels in retinal images using two-dimensional matched filters. IEEE Transactions on Medical Imaging, 1989, 8(3): 263-269. DOI: 10.1109/42.34715.

[5] Li Q, You J, Zhang D. Vessel segmentation and width estimation in retinal images using multiscale production of matched filter responses. Expert Systems with Applications, 2012, 39(9): 7600-7610. DOI:10.1016/j.eswa.2011.12.046.

[6] Kaur J, Sinha H P. Automated detection of retinal blood vessels in diabetic retinopathy using Gabor filter. International Journal of Computer Science and Network Security (IJCSNS), 2012, 12(4): 109.

[7] Tian F, Li Y, Wang J, et al. Blood vessel segmentation of fundus retinal images based on improved Frangi and mathematical morphology. Computational and Mathematical Methods in Medicine, 2021, 2021: 4761517. DOI: 10.1155/2021/4761517.

[8] Singh N P, Srivastava R. Extraction of retinal blood vessels by using an extended matched filter based on second derivative of Gaussian. Proceedings of the National Academy of Sciences, India Section A: Physical Sciences, 2019, 89: 269-277. DOI: 10.1007/s40010-017-0465-3.

[9] Cruz-Aceves I, Oloumi F, Rangayyan R M, et al. Automatic segmentation of coronary arteries using Gabor filters and thresholding based on multi-objective optimization. Biomedical Signal Processing and Control, 2016, 25: 76-85. DOI: 10.1016/j.bspc.2015.11.001.

[10] Aguirre-Ramos H, Avina-Cervantes J G, Cruz-Aceves I, et al. Blood vessel segmentation in retinal fundus images using Gabor filters, fractional derivatives, and expectation maximization. Applied Mathematics and Computation, 2018, 339: 568-587. DOI: 10.1016/j.amc.2018.07.057.

[11] Singh N P, Srivastava R. Retinal blood vessels segmentation by using Gumbel probability distribution function based matched filter. Computer Methods and Programs in Biomedicine, 2016, 129: 40-50. DOI: 10.1016/j.cmpb.2016.03.001.

[12] Frangi A F, Niessen W J, Vincken K L, et al. Multiscale vessel enhancement filtering. International Conference on Medical Image Computing and Computer-Assisted Intervention. Berlin: Springer. 1998: 1496. DOI: 10.1007/BFb0056195.

[13] Kumar D, Pramanik A, Kar S S, et al. Retinal blood vessel segmentation using matched filter and Laplacian of Gaussian. 2016 International Conference on Signal Processing and Communications (SPCOM). Piscataway: IEEE, 2016: 1-5. DOI: 10.1109/SPCOM.2016.7746666.

[14] Fathi A, Naghsh-Nilchi A R. Automatic wavelet-based retinal blood vessels segmentation and vessel diameter estimation. Biomedical Signal Processing and Control, 2013, 8(1): 71-80. DOI: 10.1016/j.bspc.2012.05.005.

[15] Zhao Y Q, Wang X H, Wang X F, et al. Retinal vessels segmentation based on level set and region growing. Pattern Recognition, 2014, 47(7): 2437-2446. DOI: 10.1016/j.patcog.2014.01.006.

[16] Rezaee K, Haddadnia J, Tashk A. Optimized clinical segmentation of retinal blood vessels by using combinationof adaptive filtering, fuzzy entropy and skeletonization. Applied Soft Computing, 2017, 52: 937-951. DOI: 10.1016/j.asoc.2016.09.033.

[17] Ghoshal R, Saha A, Das S. An improved vessel extraction scheme from retinal fundus images. Multimedia Tools and Applications, 2019, 78: 25221-25239. DOI: 10.1007/s11042-019-7719-9.

[18] Zhao Y, Rada L, Chen K, et al. Automated vessel segmentation using infinite perimeter active contour model with hybrid region information with application to retinal images. IEEE Transactions on Medical Imaging, 2015, 34(9): 1797-1807. DOI: 10.1109/TMI.2015.2409024.

[19] Rodrigues L C, Marengoni M. Segmentation of optic disc and blood vessels in retinal images using wavelets, mathematical morphology and Hessian-based multi-scale filtering. Biomedical Signal Processing and Control, 2017, 36: 39-49. DOI: 10.1016/j.bspc.2017.03.014.

[20] Rodrigues J, Bezerra N. Retinal vessel segmentation using parallel gray scale skeletonization algorithm and mathematical morphology. 29th SIBGRAPI Conference on Graphics, Patterns and Images (SIBGRAPI). Piscataway: IEEE, 2016: 17-24. DOI: 10.1109/SIBGRAPI.2016.012.

[21] Câmara Neto L C, Ramalho G L B, Rocha Neto J F S, et al. An unsupervised coarse-to-fine algorithm for blood vessel segmentation in fundus images. Expert Systems with Applications, 2017, 78: 182-192. DOI: 10.1016/j.eswa.2017.02.015.

[22] Prasanna P, Samiksha P, Ravi K, et al. Indian diabetic retinopathy image dataset (IDRiD): A database for diabetic retinopathy. Screening Research Data, 2018, 3(3): 25. DOI: 10.3390/data3030025.

[23] Liu X, Tan H, Wang W, et al. Deep learning based retinal vessel segmentation and hypertensive retinopathy quantification using heterogeneous features cross-attention neural network. Frontiers in Medicine, 2024, 11: 1377479. DOI: 10.3389/fmed.2024.1377479.

[24] Zhu H, Shu H, Luo L. Blood vessels segmentation in retina via wavelet transforms using steerable filters. Proceedings. 17th IEEE Symposium on Computer-Based Medical Systems, Bethesda. Piscataway: IEEE 2004: 316-321. DOI: 10.1109/CBMS.2004.1311734.

[25] Singh L K, Khanna M, Thawkar S, et al. Deep-learning based system for effective and automatic blood vessel segmentation from Retinal fundus images. Multimedia Tools and Applications, 2024, 83: 6005-6049. DOI: 10.1007/s11042-023-15348-3.

[26] Khanna M, Singh L K, Thawkar S, et al. Deep learning based computer-aided automatic prediction and grading system for diabetic retinopathy. Multimedia Tools and Applications, 2023, 82: 39255-39302. DOI: 10.1007/s11042-023-14970-5.

[27] Khanna M, Singh L K, Thawkar S, et al. PlaNet: A robust deep convolutional neural network model for plant leaves disease recognition. Multimedia Tools and Applications, 2024, 83: 4465-5517. DOI: 10.1007/s11042-023-15809-9.

[28] Khanna M, Agarwal A, Singh L K, et al. Radiologist-level two novel and robust automated computer-aided prediction models for early detection of COVID-19 infection from chest X-ray images. Arabian Journal for Science and Engineering, 2023, 48: 11051-11083. DOI: 10.1007/s13369-021-05880-5.

[29] Rajinikanth V, Lin H, Panneerselvam J, et al. Examination of retinal anatomical structures—A study with spider monkey optimization algorithm. Applied Nature-Inspired Computing: Algorithms and Case Studies. Berlin: Springer, 2019: 177-197. DOI: 10.1007/978-981-13-9263-4_8.

[30] Deng L, Liu S, Wang X, et al. Particle swarm optimization and salp swarm algorithm for the segmentation of diabetic retinal blood vessel images. Computional Intelligence Neuroscience, 2022, 2022(7): 1-14. DOI: 10.1155/2022/1936482.

[31] Arnay R, Fumero F, Jose S. Ant colony optimization based method for optic cup segmentation in retinal images. Applied Soft Computing, 2017, 52: 409-417. DOI: 10.1016/j.asoc.2016.10.026.

[32] Al-Rawi M, Karajeh H. Genetic algorithm matched filter optimization for automated detection of blood vessels from digital retinal images. Computer Methods and Programs in Biomedicine, 2007, 87(3): 248-253. DOI: 10.1016/j.cmpb.2007.05.012.

[33] Staal J, Abramoff M D. Ridge-based vessel segmentation

in color images of the retina. IEEE Transactions on Medical Imaging, 2016, 23(4): 501-509. DOI: 10.1109/TMI.2004.825627.

[34] Tian F, Li Y, Wang J, et al. Blood vessel segmentation of fundus retinal images based on improved Frangi and mathematical morphology. Computational and Mathematical Methods in Medicine, 2021, 2021(1): 4761517. DOI: 10.1155/2021/4761517.

[35] Janani V, Shanthi C. Infrared image enhancement using contrast limited adaptive histogram equalization and denoising convolution neural network. 2023 12th International Conference on System Modelling & Advancement in Research Trends (SMART).2023: 3-6. DOI: 10.1109/SMART59791.2023.10428573.

[36] Jerman T, Pernuš F, Likar B, et al. Beyond Frangi: An improved multiscale vesselness filter. Medical Imaging 2015: Image Processing, 2015, 9413: 623-633. DOI: 10.1117/12.2081147.

[37] Panda R, Puhan N B, Panda G. New binary Hausdorff symmetry measure based seeded region growing for retinal vessel segmentation. Biocybernetics and Biomedical Engineering, 2016, 36(1): 119-129. DOI: 10.1016/j.bbe.2015.10.005.

[38] Zhang J, Dashtbozorg B, Bekkers E, et al. Robust retinal vessel segmentation via locally adaptive derivative frames in orientation scores. IEEE Transactions on Medical Imaging, 2016, 35(12): 2631-2644. DOI: 10.1109/TMI.2016.2587062.

[39] Pandey D, Yin X, Wang H, et al. Accurate vessel segmentation using maximum entropy in corporating line detection and phase-preserving denoising. Computer Vision and Image Understanding, 2017, 155: 162-172. DOI: 10.1016/j.cviu.2016.12.005.

[40] Aguirre-Ramos H, Avina-Cervantes J G, Cruz-Aceves I, et al. Blood vessel segmentation in retinal fundus images using Gabor filters, fractional derivatives, and expectation maximization. Applied Mathematics and Computation, 2018, 339: 568-587. DOI: 10.1016/j.amc.2018.07.057.

[41] Rocha D A, Barbosa A B, Guimarães D S, et al. An unsupervised approach to improve contrast and segmentation of blood vessels in retinal images using CLAHE, 2D Gabor wavelet, and morphological operations. Research on Biomedical Engineering, 2020, 36(1): 67-75. DOI: 10.1007/s42600-019-00032-z.